

Table I. Values of $\delta_a(A)$ as given in I (first number) and by present work for the nickel isotopes.

Levels \ A	4	6	8	10
$p_{3/2}$	0.247	0.167	0.113	0.083
	0.217	0.166	0.129	0.065
$f_{5/2}$	0.139	0.184	0.207	0.199
	0.149	0.182	0.201	0.212
$p_{1/2}$	0.055	0.081	0.126	0.229
	0.069	0.095	0.136	0.212
$g_{9/2}$	0.007	0.006	0.005	0.001
	0.009	0.009	0.008	0.009

All the matrix elements of pair operators in the above equation can easily be computed up to second order in the RPA amplitudes and thus, Eq. (6) reduces to a system of linear inhomogeneous equation, to be solved for c_a .

We have taken up as examples the nickel isotopes as given in I. We start with an arbitrary set of $\delta_a(A)$, solve the gap equation for the nucleus A , and, using the RPA results, calculate a new set of $\delta_a(A)$ according to Eq. (5). Results for $\delta_a(A)$ and ground-state energies are given in Tables I and II, and are compared with those of I. We see that the trends of δ_a as function of a are identical. This fact is connected with the

Table II. Ground-state energies of the nickel isotopes.

W_0 \ A	4	6	8	10
Exact	-2.11	-1.75	-0.51	1.70
Paper I	-2.06	-1.69	-0.40	1.83
Present work	-2.02	-1.70	-0.47	1.86

first term in (5) which is given approximately by

$$c_a \langle 0(A) | s_{\alpha} a_{\alpha}^{\dagger} a_{\alpha} | 0(A-2) \rangle \sim c_a u_a(A-2) v_a(A)$$

and is largest at the level of the Fermi surface.

In conclusion, we believe that still better results can be obtained if, instead of the RPA, other methods are used to define more properly the excited states, or equivalently to calculate the matrix elements in Eqs. (5) and (6).

*Postal address: Laboratoire de Physique Théorique et Hautes Energies, Bâtiment 211, Faculté des Sciences, 91 Orsay, France.

†Laboratoire associé au Centre National de la Recherche Scientifique.

¹G. Do Dang and A. Klein, Phys. Rev. **143**, 735 (1966).

²G. Do Dang and A. Klein, Phys. Rev. **147**, 689 (1967), referred to as II. This and paper I should be consulted for notations and references.

EXCITATION OF SINGLE NEUTRON HOLE STATES IN Pb^{207} BY INELASTIC PROTON SCATTERING AT 20.2 MeV*

C. Glashauser, B. G. Harvey, D. L. Hendrie, J. Mahoney, E. A. McClatchie, and J. Saudinos†
Lawrence Radiation Laboratory, University of California, Berkeley, California
(Received 21 August 1968)

Differential cross sections for the excitation of the 0.570-, 0.894-, 1.633-, 2.33-, and 2.74-MeV states in Pb^{207} have been measured in inelastic proton scattering at 20.2 MeV. Analysis via the microscopic model indicates that core polarization is important in describing these presumed single-particle transitions.

Differential cross sections for the excitation of single-particle or single-hole states provide a direct test of the microscopic model¹⁻³ of inelastic proton scattering. Few experimental data exist, however, since the cross sections are generally much smaller than the cross sections for the excitation of collective states. Angular distributions are reported here for five such transitions in Pb^{207} at an incident proton energy of 20.2 MeV. The analysis of these data in terms of the microscopic model indicates that a large

part of the observed cross section is due to excitation of the Pb^{208} core.

The first five states in Pb^{207} , at 0.0, 0.570, 0.894, 1.633, and 2.33 MeV, are considered to be single $3p_{1/2}$, $2f_{5/2}$, $3p_{3/2}$, $1i_{13/2}$, and $2f_{7/2}$ neutron holes, respectively, in a Pb^{208} core. The $\frac{9}{2}^+$ state at 2.74 MeV has been identified as the $[2g_{9/2}, Pb^{208}(g.s.)]_{9/2^+}$ state in (d, p) reactions⁴ on Pb^{208} ; recent analysis⁵ of reactions which proceed via the analog of this state indicates a 6% admixture of the $[2g_{9/2}, Pb^{208}(2^+)]_{9/2^+}$ configura-

tion. Within the probable errors of analysis, the measured spectroscopic factors for excitation of the hole states in single-nucleon transfer reactions are appropriate for pure single-hole configurations.⁶ Further, no definite evidence from such reactions has yet been found to indicate that the hole strength is split or that Pb²⁰⁸ is not a good closed shell.

On the other hand, values⁷ of $B(E2)$ have been measured for the $(2f_{5/2})^{-1}-(3p_{1/2})^{-1}$ and $(3p_{3/2})^{-1}-(3p_{1/2})^{-1}$ transitions in Pb²⁰⁷; an effective charge close to 1 has been deduced. In addition, while the magnetic moment of the ground state of Pb²⁰⁷ is close to the Schmidt value, the magnetic moments of the $\frac{5}{2}^-$ state⁸ in Pb²⁰⁷ and the ground state of Bi²⁰⁹ differ considerably from the single-particle limits. Values of $B(E2)$ derived from the measured quadrupole moment of Bi²⁰⁹ and from Coulomb excitation of the $(2f_{7/2})^1$ proton state in Bi²⁰⁹ give an effective charge of the extra-core proton of about 2 or even larger. Contrary to the evidence from transfer reactions, these data indicate there is considerable polarization of the Pb²⁰⁸ core.

The present inelastic scattering data were taken with the 20.2-MeV proton beam of the Berkeley 88-in. cyclotron; no analog-state resonances have been found at this energy.⁹ Two 3-mm Si(Li) detectors were used; an overall resolution of about 30 keV was maintained in each. A ratio of peak channel elastic counts to nearby background of about 10⁴ was obtained by careful beam preparation and choice of counter collimators. Because of the small Pb²⁰⁷ cross sections, light-element contaminants¹⁰ in the target were a major problem; at some angles, these contributed the largest components of the experimental error. Absolute cross sections correct to about $\pm 5\%$ were obtained by comparing the measured elastic cross sections with optical-model predictions.

The resulting differential cross sections are shown in Fig. 1, together with theoretical curves described below. Five sets of optical parameters were obtained which gave good fits to the elastic scattering data; they are given in Table I. The set used in calculating the curves illustrated is the first set listed in the table. The microscopic-model calculations assumed a direct (D)

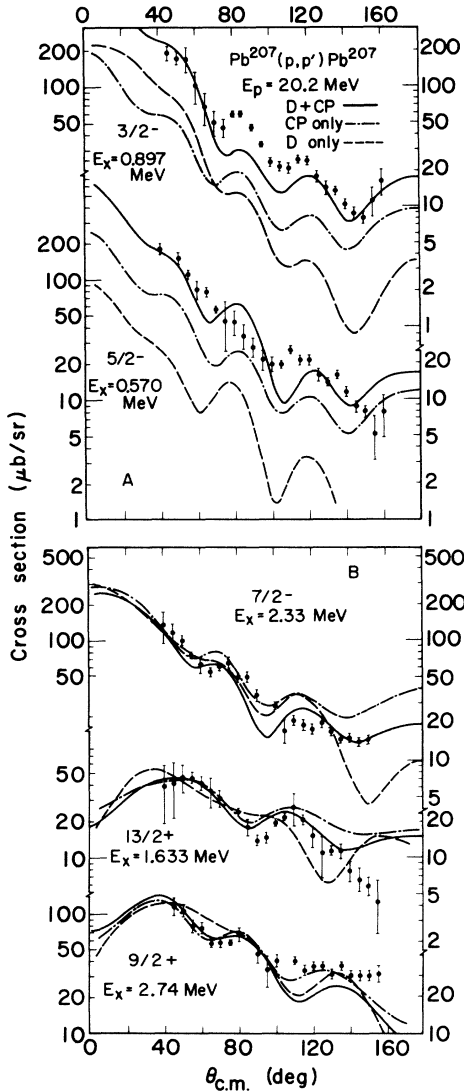


FIG. 1. (a) Measured cross sections and predictions of the microscopic model. The label D refers to the direct or single-particle cross section alone; the label CP refers to the core-polarization cross section alone. The D + CP calculations include the coherent contributions of each. The normalization of all curves assumes the D + CP values of Table II. (b) The solid curves are normalized as in (a). The normalizations of the D and CP curves are adjusted to give the best fit to the data.

Table I. Parameters of the optical potential used in the present calculation.

V_0 (MeV)	r_0 (F)	a_0 (F)	W_D (MeV)	r_I (F)	a_I (F)	V_{s0} (MeV)	r_{s0} (F)	a_{s0} (F)
52.62	1.25	0.65	9.69	1.25	0.76	6.38	1.25	0.65
57.24	1.184	0.74	8.38	1.38	0.73	6.31	1.12	0.60
52.14	1.25	0.65	8.62	1.29	0.76	6.38	1.25	0.65
57.52	1.20	0.70	11.27	1.25	0.70	6.37	1.10	0.70
62.71	1.12	0.75	9.28	1.33	0.75	6.3	1.12	0.75

projectile-target-nucleus interaction of the standard form:

$$V_{ij}(r_{ij}) = (V_0 + V_1 \sigma_i \sigma_j) g(|r_{ij}|);$$

a Yukawa shape with range 1 F was chosen for $g(|r_{ij}|)$. The strength of the potential V_1 , which allows transfer of spin angular momentum (S) to the target, was set to $\frac{1}{3}V_0$. A nonlocality range of 0.85 F was assumed in the computation of bound-state wave functions; the curves shown do not include nonlocality in the distorted waves. The depth of the bound-state Woods-Saxon well was adjusted to give the correct binding energy; the radius was $1.20A^{1/3}$ F and the diffuseness was 0.7 F. Antisymmetrization of the projectile with the target nucleons was not included.

Predictions¹¹ of this model are shown by the dashed curves in Fig. 1. The values of V_0 obtained by normalizing these curves to give the best fit to the experimental data are listed in Table II. [This is the normalization illustrated in Fig. 1(b).] Note that the strengths are much larger than the free proton-neutron interaction strength although they are comparable with the values found in other similar microscopic-model analyses in even-even nuclei.^{1,12}

In computing the D cross sections, $S=1$ contributions were included only for the minimum orbital (L) and total (J) angular momentum transfer allowed. These $S=1$ contributions are substantial for all states except the $\frac{5}{2}^-$ state, but $S=1$ contributions for larger values of L and J are not significant. The values of $V_0(D)$ in

Table II are subject to some uncertainty because of the poor quality of the fits. Uncertainties arise also from ambiguities in the parameters of the optical and bound-state potentials and in the range of the force. However, further calculations were performed with the four other optical potentials; the range of the force was varied between 0.7 and 1.4 F and the radius of the bound-state well was varied between 1.1 and $1.35A^{1/3}$ F. These calculations indicate that no reasonable change in these parameters will reduce $V_0(D)$ by more than about 30%.

These strengths might be lowered significantly if the knockout-exchange amplitudes were included. Recent calculations by Atkinson and Madsen¹³ indicate that the exchange and direct amplitudes are closely in phase, that the relative cross section is affected mostly at large angles, and that the ratio of total cross sections $\sigma(\text{exchange})/\sigma(\text{direct})$ increases rapidly with L . Assuming a Serber exchange mixture for a force of Yukawa shape, they have calculated this ratio for the $[(1g_{9/2})^2]_{0+} - [(1g_{9/2})^2]_{2+}$ proton transitions in Zr⁹⁰. Their results can give a rough guide¹³ to the exchange contributions to the Pb²⁰⁷ transitions. They indicate that the values of V_0 might all be reduced to about 100 MeV, which is about twice as large as the free nucleon-nucleon scattering strength.

The fact that the values generally found for V_0 are so large has led Love and Satchler¹⁴ to develop a way of treating core-polarization effects. In their phenomenological model, which does not include exchange contributions, the effects of

Table II. Strength parameters. The values $V_0(D)$ were derived without core polarization. The parameters $V_0(D+CP)$, $\langle r^L \rangle$, and e_{eff} were used in the core polarization calculations. The parameter R_c is $1.2A^{1/3}$ F.

State	L	S	J	$V_0(D)$	$V_0(D+CP)$	$\langle r^L \rangle / R_c^L$	e_{eff}
5/2 -	2	0	2	160 MeV	60 MeV	0.62	1.0
	2	1	2				
3/2 -	2	0	2	110	60	0.71	1.0
	0	1	1				
13/2 +	7	0	7	285	60	0.84	0.73
	5	1	6				
7/2 -	4	0	4	170	60	0.75	1.0
	2	1	3				
9/2 +	5	0	5	175	60	1.10	0.75
	3	1	4				

collective correlations neglected in the nuclear wave functions are included by coherently adding to the direct form factor a core-polarization form factor (CP). The strength of the CP term is proportional to the value of $B(E1)$. In transitions for which $B(E1)$ has been previously determined, e.g., the $(3p_{1/2})^{-1}-(3p_{3/2})^{-1}$ and $(3p_{1/2})^{-1}-(2f_{5/2})^{-1}$ transitions in Pb^{207} , including the CP term does not add a free parameter to the calculation. For other transitions $B(E1)$ can be determined from the inelastic scattering data provided V_0 is fixed.

Calculations of this type for transitions with known $B(E2)$ are shown by the solid curves in Fig. 1(a). The quality of the fits to the shapes of the experimental distributions are generally improved, although it is interesting that the pure CP fits (the dotted curves) are better. The magnitudes of the cross sections predicted by the microscopic model for these first two transitions are now in reasonable agreement with the data. The value of V_0 is 60 MeV, which is close to the free nucleon-nucleon interaction. Note that the cross section predicted with the CP term alone is almost everywhere larger than the cross section predicted with the D term alone. The fact that the CP term alone is not sufficient, however, indicates that the $B(E1)$ which would be derived from a purely collective-model analysis of these data (without exchange contributions) would not be consistent with the $B(E1)$ derived from electromagnetic data.

With V_0 fixed at 60 MeV, D+CP calculations for the higher states [the solid curves of Fig. 1(b)] determine $B(E1)$ for these transitions; from $B(E1)$, values of the effective charge¹⁴ were deduced. The radial matrix elements $\langle f | r^L | i \rangle$ needed to determine e_{eff} were evaluated with the same Woods-Saxon wave functions used in the scattering calculations. These values of $\langle r^L \rangle$ (cf. Table II) are up to three times larger than those used in defining Weisskopf units.¹⁵ For all these higher transitions the CP contribution is substantially larger than the D contribution, but the relative importance of the two terms could

change if exchange were included. The values of e_{eff} calculated without exchange are shown in Table II.

*Work supported by the U. S. Atomic Energy Commission.

†Present address: Service de Physique Nucléaire à Moyenne Energie, Centre d'Etudes Nucléaires de Saclay, Gif-sur-Yvette, Seine et Oise, France.

¹N. K. Glendenning and M. Veneroni, *Phys. Rev.* **144**, 839 (1966).

²G. R. Satchler, *Nucl. Phys.* **77**, 481 (1966); K. A. Amos, V. A. Madsen, and I. E. McCarthy, *Nucl. Phys.* **A94**, 103 (1967).

³G. Vallois, thesis, University of Paris, 1967 (unpublished); C. B. Fulmer, J. B. Ball, A. Scott, and M. L. Whiten, *Phys. Letters* **24B**, 505 (1967); M. M. Stautberg, J. J. Kraushaar, and B. W. Ridley, *Phys. Rev.* **157**, 977 (1967).

⁴P. Mukherjee and B. L. Cohen, *Phys. Rev.* **127**, 1284 (1962); W. Darcey, A. F. Jeans, and K. N. Jones, *Phys. Letters* **25B**, 599 (1967).

⁵N. Auerbach and N. Stein, *Phys. Letters* **27B**, 122 (1968).

⁶G. Muehlehner, A. S. Poltorak, W. C. Parkinson, and R. H. Bassel, *Phys. Rev.* **159**, 1039 (1967); W. C. Parkinson, D. L. Hendrie, H. H. Duham, J. Mahoney, J. Saudinos, and G. R. Satchler, to be published.

⁷Cf. O. Nathan and S. G. Nilsson, *Alpha-, Beta-, and Gamma-Ray Spectroscopy*, edited by Kai Siegbahn (North-Holland Publishing Company, Amsterdam, The Netherlands 1965), p. 601.

⁸S. Gustaffson, K. Johannsson, E. Karlsson, and A. G. Svensson, *Phys. Letters* **10**, 191 (1964).

⁹N. Stein, private communication.

¹⁰The contaminants (Na, Si, Al, P, S, and Cl) appear to come from the commercial detergent Teepol that was used to facilitate stripping of the target foils from the glass substrate on to which they were evaporated.

¹¹We are grateful to A. D. Hill and P. D. Kunz for making their computer codes available to us.

¹²G. R. Satchler, *Nucl. Phys.* **A95**, 1 (1967).

¹³Jay Atkinson and V. A. Madsen, *Phys. Rev. Letters* **21**, 295 (1968); V. A. Madsen, private communication.

¹⁴W. G. Love and G. R. Satchler, *Nucl. Phys.* **A101**, 424 (1967).

¹⁵J. M. Blatt and V. F. Weisskopf, *Theoretical Nuclear Physics* (John Wiley & Sons, New York, 1952), p. 626.